Proceedings of the ASME TURBO EXPO 2015 Gas Turbine Technical Congress & Exposition
TURBO EXPO 2015
June 15-19, 2015, Montreal, Canada

GT2015-42399

ASSESSMENT OF THE INDIRECT COMBUSTION NOISE GENERATED IN A TRANSONIC HIGH-PRESSURE TURBINE STAGE

Dimitrios Papadogiannis *
Florent Duchaine
Laurent Gicquel
CFD team
CERFACS
42 ave Gaspard Coriolis
31057, Toulouse, France
Email: dimitrios.papadogiannis@cerfacs.fr

Gaofeng Wang
Stéphane Moreau
Département de Génie Mécanique
University of Sherbrooke
Sherbrooke, Québec, J1K 2R1
Canada

Franck Nicoud
CNRS UMR 5149
Université de Montpellier II
Place Eugène Bataillon, 34095, Montpellier
France

ABSTRACT

Indirect combustion noise, generated by the acceleration and distortion of entropy waves through the turbine stages, has been shown to be the dominant noise source of gas turbines at low-frequencies and to impact the thermoacoustic behavior of the combustor. In the present work, indirect combustion noise generation is evaluated in the realistic, fully 3D transonic high-pressure turbine stage MT1 using Large-Eddy Simulations (LES). An analysis of the basic flow and the different turbine noise generation mechanisms is performed for two configurations: one with a steady inflow and a second with a pulsed inlet, where a plane entropy wave train at a given frequency is injected before propagating across the stage generating indirect noise. The noise is evaluated through the Dynamic Mode Decomposition of the flow field. It is compared with previous 2D simulations of a similar stator/rotor configuration, as well as with the compact theory of Cumpsty and Marble. Results show that the upstream propagating entropy noise is reduced due to the choked turbine nozzle guide vane. Downstream acoustic waves are found to be of similar strength to the 2D case, highlighting the potential impact of indirect combustion noise on the overall noise signature of the engine.

*Address all correspondence to this author.

NOMENCLATURE

w^+ Downstream propagating acoustic wave
w^- Upstream propagating acoustic wave
w^s Entropy wave
p Pressure
ρ Density
c Speed of Sound
γ Heat capacity ratio
u_p Wave convection velocity
LES Large Eddy Simulation
EWF Entropy Wave Frequency
BPF Blade Passing Frequency
DMD Dynamic Mode Decomposition
SPDMD Sparsity-Promoting Dynamic Mode Decomposition
CFD Computational Fluid Dynamics

INTRODUCTION

Combustion noise is the low-frequency noise generated in the combustion chamber of gas turbines and comes from two main mechanisms. On the one hand, direct noise emanates from the acoustic waves created at the unsteady flame front and propagated through the rest of the engine at the speed of sound plus the convection velocity. On the other hand, the unsteady combustion also gives rise to low-frequency temperature fluctuations, or entropy waves, that are convected with the flow velocity to the

Copyright © 2015 by ASME

combustor nozzle and turbine, where they are accelerated and distorted, generating acoustic waves. This is the indirect noise generation mechanism and its importance is twofold: first it increases the noise signature of the engine and secondly, the acoustic waves propagating upstream can impact the thermoacoustic behavior of the combustion chamber [1]. Yet its actual relevance and relative importance with respect to the direct combustion noise remains controversial.

Due to the complexity of a full 3D high-pressure turbine, past theoretical and numerical studies of the phenomenon have used simplified turbine-like geometries. The first in-depth analyses on turbine-like geometries focused on the propagation of entropy waves through quasi-1D nozzles. Marble and Candel [2] developed an analytical method to evaluate the transmission coefficients of acoustic and entropy waves propagating through a compact quasi-1D nozzle, its length being significantly smaller than the wavelength of the incoming waves. More recently, Duran and Moreau [3] proposed an analytical method to calculate the transmission coefficients of general quasi-1D nozzles, removing the compact nozzle assumption. These analytical methods, accompanied by numerical predictions from LES, have been evaluated on the experimental Entropy Wave Generator [4], with [5] reporting good agreement.

The theory of Marble and Candel for nozzles has been extended to 2D compact blade rows [6], taking into account the turning of the flow. This is achieved by imposing an additional constraint, the Kutta condition at the blade trailing edge. The method, originally conceived for a single blade row, was also extended to multi-stage turbines and has been compared against simulations of a 2D high-pressure turbine stage [7, 8].

The present work is the first numerical evaluation of the indirect combustion noise generated in a realistic, fully 3D, transonic single-stage high-pressure turbine. A train of sinusoidal entropy waves of constant frequency and amplitude is injected to model the entropy waves generated in a combustor. For this study, the Dynamic Mode Decomposition (DMD) is employed for the analysis of the flow field [9]. First, the global spectra of the forced case are investigated against a steady inflow case to evaluate the impact of the waves on the noise generation of the turbine. Afterwards, the response of the flow field at the pulsation frequency for the forced case is examined using DMD and transmission coefficients are obtained for the generated acoustic waves. Finally, the results are compared to those obtained with the 2D theoretical model of [6].

NUMERICAL SET-UP

The transonic single-stage MT1 turbine [10], consisting of 32 stator and 60 rotor blades, is chosen for this study. In an effort to find a reduced periodic domain for the simulations and control the computational cost, the "reduced blade count" technique is employed at the stator blade row [10]. It results in a domain with 30 stator blades and 60 rotors so a periodic domain with 1 stator and 2 rotors can be simulated (12 degree periodicity) instead of the full annulus. The mean predicted aerodynamic flow field of this scaled configuration has already been extensively validated against experimental measurements [11, 12].

Numerical schemes

Performing LES of turbomachinery stages requires careful treatment of the rotor/stator interactions. To this end, the Multi Instances Solvers Coupled via Overlapping Grids (MISCOG) method is employed [13], where two instances of the reactive LES solver AVBP are coupled through the OpenPALM coupler [14]. The first instance computes the flow field across the stator, while the second one handles the moving blades of the turbine. The numerical integration is handled in all simulations by the two-step, finite-element TTGC [15] scheme that is 3rd order accurate in time and space and explicit in time. This scheme is used in conjunction with Hermitian interpolation for the data exchange at the overlap zone, ensuring low dissipation and low dispersion of the rotor/stator interactions, while preserving the global order of accuracy of the employed numerical scheme.

Mesh and Modeling

A fully 3D hybrid mesh is used, with 10 prismatic layers around the blades and tetrahedral elements in the passage and endwalls. It is composed of 9.4 million cells in total for the stator domain and 21 million cells for the rotor domain. It is also designed to place the first nodes around the blade walls in the logarithmic region of a turbulent boundary layer. The first cells of the wall have a maximum $\Delta y^+ = 50$. The prisms have a low aspect ratio set to $\Delta x^+ \approx \Delta z^+ \approx 4\Delta y^+$, permitting a good resolution of streamwise/spanwise flow. The rotor tip region contains approximately 17 cell layers, yielding a relatively limited resolution in that region but providing a reasonable time step. Sub-grid scale closure relies on the WALE model [16]. Figure 1 provides a view of the mesh of the stator and rotor at mid-span (Figs. 1a and 1b) and of the refinement at the rotor tip (Fig. 1c). The axial direction follows of the X axis.

Boundary and operating conditions

The boundary conditions follow the non-reflecting Navier-Stokes Characteristic Boundary Conditions (NSCBC) formulation [17]. At the inlet the total temperature and total pressure are imposed, while at the outlet the static pressure is specified. Note that no turbulent fluctuations are added at the inlet, as only the pure indirect combustion noise generated in the turbine is investigated. For the forced simulations, sinusoidal entropy spots are introduced through the corresponding characteristic equation. The frequency of the imposed waves is 2 kHz and the amplitude equal to 4.8% of the inlet total temperature. While combustion noise

Copyright © 2015 by ASME

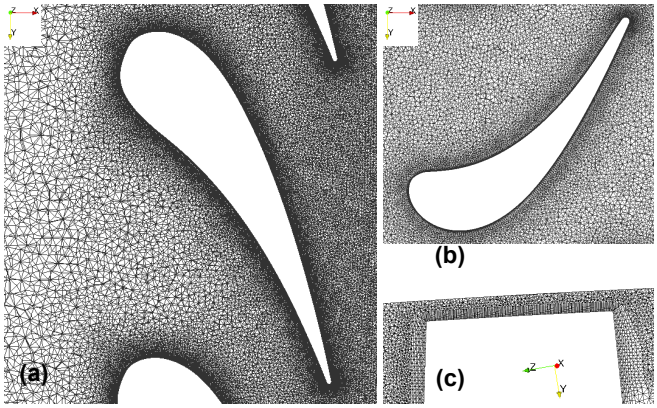

FIGURE 1: MESH VIEW OF THE STATOR AT MID-SPAN (a), OF THE ROTOR AT MID-SPAN (b) AND AT THE ROTOR TIP (c)

Rotational Speed (rpm)	9500
Inlet total pressure (Pa)	$4.56e5$
Inlet total temperature (K)	444
Mass flow (kg/sec)	17.4
Outlet static pressure (Pa)	$1.4e5$
Wave amplitude (K)	20
Wave frequency (Hz)	2000

TABLE 1: OPERATING CONDITIONS OF THE MT1 TURBINE

is usually associated to lower frequencies, 2 kHz was found to be approximately the limit of the validity of the compact theory in 2D configurations and renders the simulations more affordable. The reduced frequency of the forcing is $\Omega = fL_n/c_0 = 0.1$, with L_n being the rotor chord length, f the forcing frequency and c_0 the speed of sound at the turbine inlet. Due to the complexity of this high Reynolds transonic 3D turbine, a monochromatic pulsation is preferred over a more realistic broadband pulsation in an effort to facilitate distinguishing pure indirect noise from other sources of noise. The operating and boundary conditions employed in this work are summarized in Table 1.

RESULTS

Overall flow topology

The overall flow topology is first analyzed for the two cases. Looking at the full 3D field, a particularly complex flow field is revealed. Figure 2 shows density gradient contours of the flow

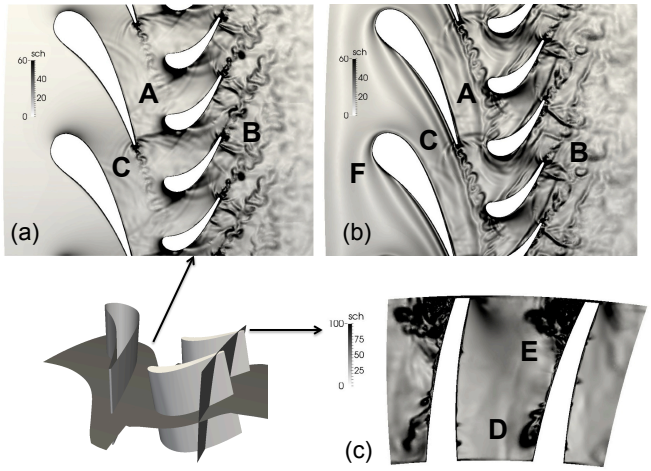

FIGURE 2: $\frac{|\nabla\rho|}{\rho}$ OF AN INSTANTANEOUS SOLUTION AT MID-SPAN FOR THE STEADY INFLOW (a) AND PULSED CASES (b) AND AT AN X-NORMAL PLANE NEAR THE ROTOR EXIT FOR THE STEADY INFLOW CASE (c)

across a cylindrical cut at mid-span of the turbine for the steady inflow and pulsed cases (Figs. 2a and 2b respectively) complemented with a view at an x-normal plane near the rotor trailing edge for the steady inflow case (Fig 2c). Some of the phenomena highlighted in Fig. 2 are the shock/boundary layer interaction on the suction side of both the stator and the rotor (positions A and B), vortex shedding from the trailing edge of the blades and the accompanying acoustic waves emitted (position C), as well as strong secondary flows developing at the endwalls (positions D and E). For the pulsed case (Fig. 2b), on top of the previously highlighted phenomena, the planar entropy waves approaching the stator are also evidenced (position F). As they go through the stator passages they get distorted and partially mixed by the blade wakes before being cut by the passing rotors. The mixing and the developing turbulence make the entropy waves less visible in the rotor domain, highlighting the difficulty of working on unprocessed LES data.

0.1 Dynamic Mode Decomposition of the LES flow field

A frequency domain analysis is performed by applying the Dynamic Mode Decomposition (DMD) to a set of instantaneous flow fields. DMD utilizes a number of flow snapshots, obtained at a constant sampling frequency, and decomposes the flow field in different modes, each with a unique frequency. It is particularly efficient in identifying single-frequency oscillatory motions, such as acoustic waves that are of interest for this study. The DMD has been selected here compared with other

Copyright © 2015 by ASME

frequency-domain methods because it is robust and can provide information on the frequency content of the flow having resolved fewer periods per frequency of interest, thereby reducing the overall simulation cost. Additionally, the frequency of the computed modes does not need to be a multiple of the sampling frequency. To obtain converged and accurate turbulent statistics, especially in the highly turbulent rotor-blade wake, both the steady inflow and the pulsed simulations ran for a total of 10 periods of the pulsation frequency. To avoid aliasing, the sampling frequency needs to be high enough to include all the important high-frequency phenomena. In this case the vortex shedding from the stator trailing edge is the most significant and resolving it, as well as its first harmonic, is necessary. The necessary sampling frequency was determined to be 120kHz using a simple FFT of a temporal signal recorded at a probe in the stator wake. Since DMD is memory consuming, the decomposition is performed at cylindrical blade-to-blade planes at mid-span with the signal including the six principal primitive variables: pressure, temperature, the three velocity components and density. For the pulsed case, a set of x-normal planes at the inlet and outlet of the turbine stage is also employed to measure the incoming/outgoing acoustic and entropy waves as well as the transmission coefficients.

Figures 3 and 4 show respectively the DMD of temperature and pressure spectra of the flow in the stator (left) and rotor (right) domains (azimuthal cuts) for the stationary and forced LES. For this configuration, the Blade Passing Frequency (BPF) is 9.5 kHz and 4.75 kHz respectively for each domain. The depicted frequency ranges of Figs 3 and 4 cover respectively for the stator and the rotor, the low frequency phenomena, BPF as seen in each domain, and the first high frequency mode issued by the interaction of the BPF and the forced Entropy Wave Frequency (EWF) at 2 kHz. For the steady inflow case, Figs. 3 and 4 reveal that there is no mode at the pulsation frequency, only some low amplitude modes around the chosen forcing value are present. For the forced LES, pure entropy waves are injected, which create a distinctive peak in Fig. 3, seen both in the stator and rotor domains. Furthermore and although no acoustic forcing is imposed by the entropy waves, Fig. 4 reveals that a pressure mode with a distinctive peak appears. This indicates that acoustic waves have been generated, confirming the indirect noise generation mechanism. The imposed EWF also leads to the appearance of interaction modes between the BPF and this forcing, with noticeable pressure peaks arising at $BPF \pm EWF$. This type of interaction between combustion noise and rotor/stator tones, yielding scattered tones, has also been measured on full scale engine tests [18].

The mode of primary interest obtained by DMD corresponds to the one at the EWF. Its spatial form can be visualized to identify the spatial activity at the origin of the EWF pressure peaks present in the of Figs. 3 and 4. The modulus and phase of temperature, as well as pressure of the DMD mode are depicted in Fig. 5 at mid-span. The temperature modulus at the inlet (Fig. 5a) is practically uniform and equal to 20K, corresponding to the plane entropy waves injected in the domain. The phase at the same position (Fig. 5b) indicates that the waves in this area are simply convected by the flow and stay planar. Downstream in the blade passage, the modulus gets distorted with a reducing maximum value, as was found in previous 2D propagation studies in a stator [5] and in a turbine stage [3]. The phase also reveals an asymmetric distortion of the planar waves. This distortion is caused by the strong flow acceleration and turning imposed by the blades. An azimuthal component in the velocity is created, with the higher velocity near the suction side resulting in asymmetric propagation velocities across the azimuthal coordinate. In the rotor domain, due to the rotation, the blades see rather uniform entropy waves, with the phase at the rotor inlet being practically planar and perpendicular to the axial direction. As these waves pass through the rotors, they get deformed in a similar fashion as in the first blade row. Such strong distortions of the injected entropy wave at both the stator and the rotor leads to scattering in additional azimuthal modes. This energy redistribution mechanism can explain the arising peaks observed in the pressure and temperature spectra of Figs 3 and 4.

As anticipated in the discussion based on Figs. 3 and 4, convected temperature spots generate pressure waves in both rows at the forcing frequency. The pressure modulus and the phase of the DMD mode at EWF, pictured in Figs. 5c and 5d, reveal a complex pressure field. A significant peak of the modulus exists between the suction side at 20% chord length and the trailing edge on the pressure side, as the domain is periodic in the azimuthal direction (position 1). In this area the phase hardly changes (Fig. 5d), suggesting an excited cavity mode that stays confined between the blades, rendering it irrelevant to combustion noise. The second area of high pressure modulus can be observed on the suction side close to the trailing edge (position 2), with the sharpest peak corresponding to a shock. In the rotor domain, both the pressure modulus and phase appear to simply follow the flow, with a smooth change of phase throughout indicating simple wave propagation. To finish, a large peak in the modulus at the trailing edge of the blade corresponds to another trailing edge shock (position 3). At the outlet, the acceleration of the temperature spots through the rotor and the acoustic waves generated in the stator and transmitted in the rotor are strong enough to yield a significant pressure trace (non-zero modulus) that sticks above the broadband level. All these features identified in the stator and rotor domains are at the root of the indirect combustion noise emitted and will be quantified later in this work.

Convergence of the Dynamic Mode Decomposition

One of the advantages of DMD is the quick convergence of the method, particularly when dealing with oscillatory motions [9, 19]. The case of 3D turbine stage, however, is much more complex. While the phenomenon of interest consists of os-

Copyright © 2015 by ASME

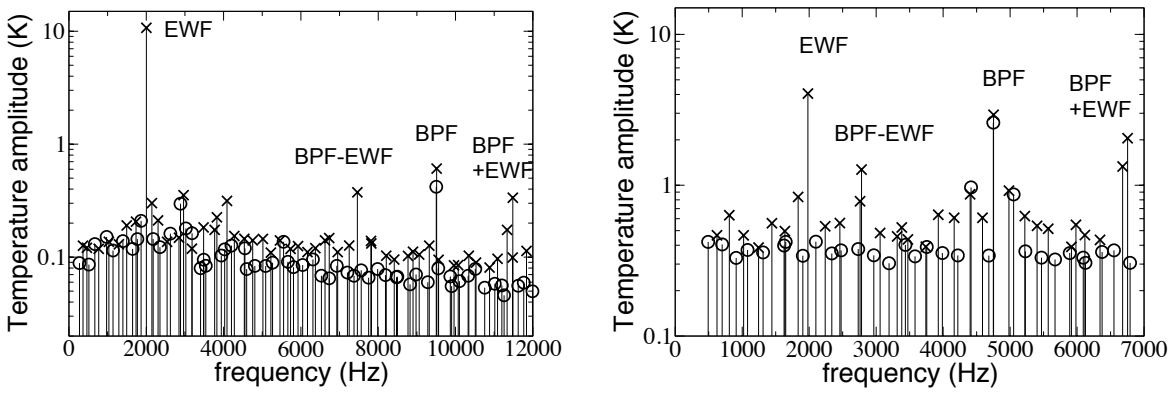

FIGURE 3: DMD SPECTRA OF TEMPERATURE FOR THE STATOR (LEFT) AND ROTOR (RIGHT) DOMAINS AT MID-SPAN - STEADY INFLOW CASE ($\circ$) AND PULSED CASE ($\times$)

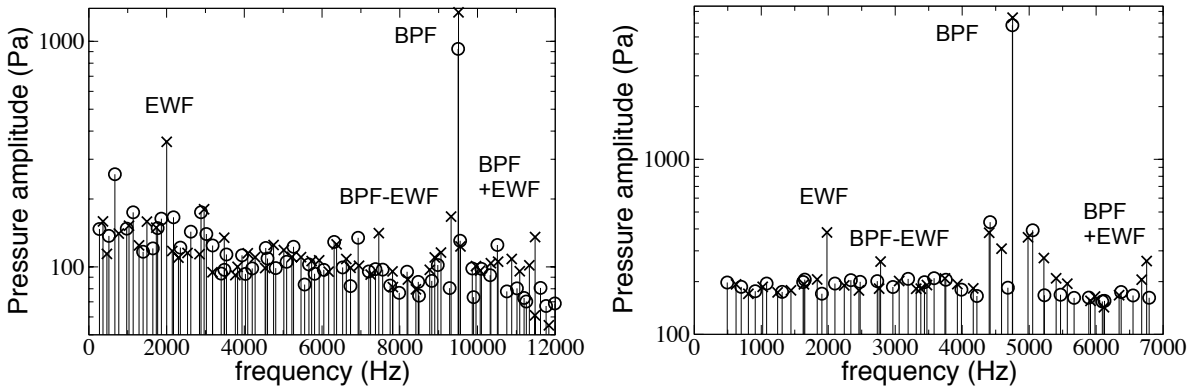

FIGURE 4: DMD SPECTRA OF PRESSURE FOR THE STATOR (LEFT) AND ROTOR (RIGHT) DOMAINS AT MID-SPAN - STEADY INFLOW CASE ($\circ$) AND PULSED CASE ($\times$)

cillating acoustic and entropy waves of a known frequency, it coexists with broadband turbulence, shocks, blade wakes, boundary layers and secondary flows, which could alter the convergence behavior of the DMD. To evaluate this potential source of uncertainties, DMD on the pulsed case at mid-span is performed with a varying number of snapshots and the same constant sampling frequency.

Figures 6 and 7 depict the DMD temperature and pressure spectra of the pulsed case for five different simulation runtimes, each equal to a multiple of the period $T = \frac{1}{EWF}$, which relates to the primary frequency of interest in this work. The sampling frequency for the snapshots is constant and equal to 120 kHz, as in the previous section. The first conclusion that can be drawn is that for the EWF amplitude there is a good agreement for all run times above $3T$. For a run time of $1T$, EWF in the stator is found to be shifted to slightly above 2 kHz, while in the rotor domain no mode at 2kHz is present. Regarding the BPF mode, a relatively good agreement is also observed, particularly above runtimes of $6T$. More important differences appear for the interaction modes $BPF \pm EWF$, where a trend of reduced pressure amplitudes appears as run-time increases. Regarding the overall spectra, it can be observed that as more snapshots are added to the signal, the amplitudes of the modes with irrelevant frequencies drop. This indicates that non-coherent broadband phenomena, such as turbulent fluctuations, are present and should not be interpreted as coherent significant modes. For the cases with $1T$ and $3T$ total runtime, for example, there are several notable peaks that either disappear or are largely reduced when more snapshots are added. For the EWF, where combustion noise will occur, 6 periods T of run-time and above appear adequate for the method to converge.

Copyright © 2015 by ASME

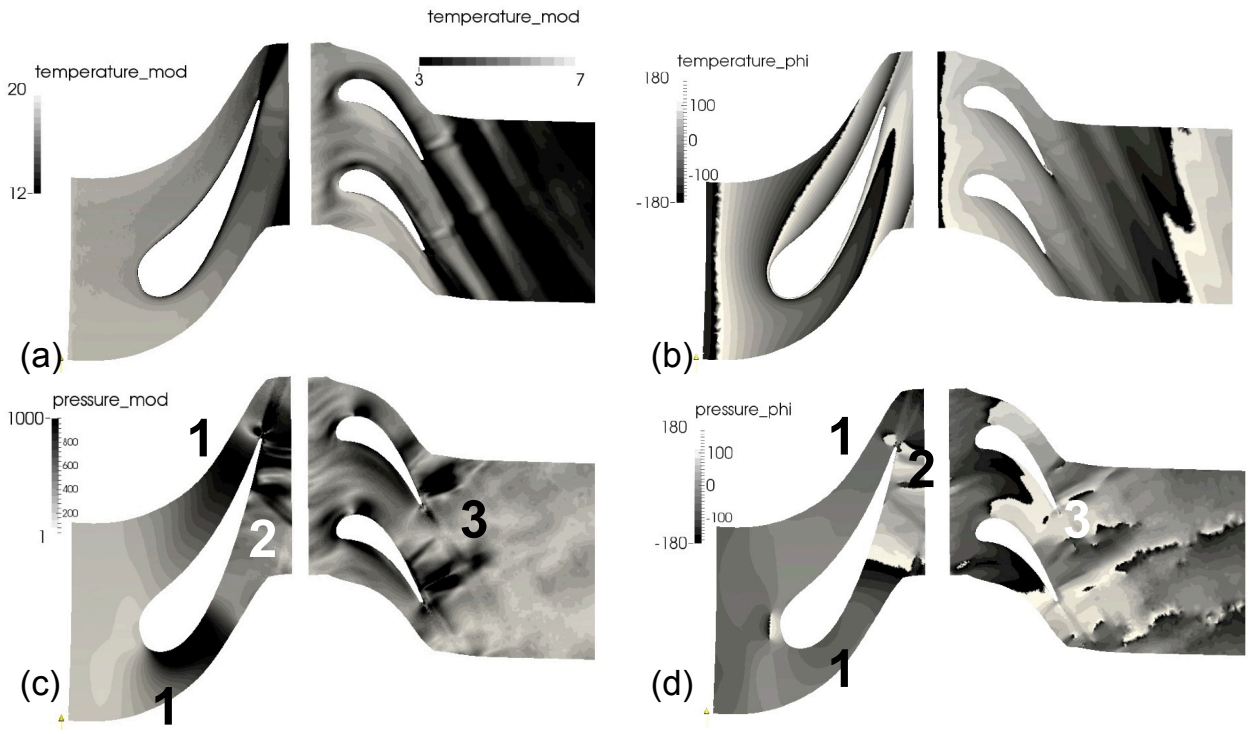

FIGURE 5: DMD 2KHZ MODE AT MID-SPAN - MODULUS AND PHASE OF THE TEMPERATURE (A AND B) AND PRESSURE (C AND D) RESPECTIVELY

Sparsity-Promoting Dynamic Mode Decomposition

The spectra of Figs. 3 and 4 reveal that several other modes are also present around the EWF. Considering this with the fact that the amplitudes of irrelevant modes can require a large amount of snapshots to converge, it is desirable to be able to evaluate the most important contributions in terms of noise generation and clean up the spectra. To do so automatically a modified version of the DMD has been developed, called the Sparsity-Promoting DMD (SPDMD) [20]. It aims at selecting the long-standing coherent modes that generate noise and remove the fast decaying ones, by a user-defined regularization parameter that controls the balance between accuracy and a dataset with a reduced set of modes.

In the following, the SPDMD is performed on pressure using the same set of instantaneous flow fields as in the previous sections, to identify the most important noise-generating modes of the flow. Figure 8 depicts the original pressure DMD spectrum with all the modes present complemented by the sparsity-promoting spectrum superimposed for the turbine inlet and outlet respectively. Both diagnostics provided in Fig. 8 are measured at the x-normal inlet and outlet planes for the pulsed case, as it is where the combustion noise will be measured. It can be seen that at the stator inlet the algorithm keeps only the pulsation mode, as expected. At the rotor exit, even though many more modes exist (caused by the local high turbulence levels), the mode corresponding to the BPF and the pulsation frequency are chosen as the most coherent ones. It can further be noted that the algorithm retains this 2 kHz mode, despite its weak amplitude. This result highlights the importance of the indirect combustion noise with respect to other flow phenomena. It also shows that SPDMD can be an appealing method for the analysis of combustors, as it has the potential of quickly identifying the entropy modes that are most probable to generate indirect noise.

Quantifying the indirect noise and comparisons with the compact theory

The noise that is measured in this study is the result of a pulsated, realistic 3D turbine with several technological effects present (notably the secondary flows at the hub and casing of the stator, the tip leakage flow at the rotor, the complete 3D shock structures and the shock-boundary layer interactions). In terms of noise generation, it can be compared with the 2D compact theory of Cumpsty and Marble. Numerical results from 2D simulations of a simplified turbine stage published in [3]. They are 2D pseudo-LES of the MT1 turbine at mid-span using the same nu-

Copyright © 2015 by ASME

merical solver as in this manuscript. While the operating point of that investigation was subsonic, compared to the transonic conditions of real high-pressure turbines, the results can serve as an additional complement between the theory and the full 3D simulations. It is worth noting that Duran et al [3] commented that 2 kHz is approximately the limit after which the compact assumption is not valid.

To measure the transmission of the generated acoustic waves, DMD is performed at the inlet and outlet x-normal planes. Assuming that at these locations the dimensionless waves are 1D plane waves, the downstream propagating acoustic wave can be calculated as $w^+ = \frac{p'}{\overline{\gamma p}} + \frac{u'}{\overline{c}}$, the upstream propagating acoustic wave as $w^- = \frac{p'}{\overline{\gamma p}} - \frac{u'}{\overline{c}}$ and the entropy wave $w^s = \frac{p'}{\overline{\gamma p} - \frac{\rho'}{\overline{\rho}}}$. The overline in these expressions indicates time averaged quantities, the prime indicates fluctuations and the heat capacity ratio γ is assumed to be constant throughout, while u indicates the axial component of the velocity. The transmission coefficients of interest are the entropy wave attenuation $Ts = \frac{w_2^s}{w_1^s}$, the acoustic wave reflection $Ra = \frac{w_1^-}{w_1^s}$ and the acoustic wave transmission $Tr = \frac{w_2^+}{w_1^s}$, with the subscript 1 indicating the turbine inlet, the subscript 2 referring to the turbine outlet and w_1^s is the forced entropy wave imposed at the inlet.

The procedure to construct the characteristic waves and measure the transmission coefficients at the inlet and outlet of the turbine stage can be decomposed in 5 steps:

1. Perform DMD of the principal flow variables at an x-normal plane both at the inlet and outlet of the turbine.
2. Isolate the mode of interest (2 kHz in this case) and form the temporal fluctuations of the variables.
3. For each point in the plane construct the 1D plane waves using the reconstructed fluctuations and a time-averaged solution.
4. Perform surface averaging and calculate the transmission coefficients.

Applying this procedure at the inlet of the turbine stage is straightforward, since there is no free-stream turbulence imposed. However, as the flow goes through the turbine it generates broadband fluctuations. While DMD allows an easy filtering of all irrelevant frequencies, turbulence or hydrodynamic phenomena whose frequency coincides with the pulsation frequency will be present in the signal and can therefore modify the evaluation of the transmission coefficients. As a result, at the rotor outlet an extra step is added before step (4): a hydrodynamic filtering based on the Characteristics Based Filtering (CBF) method [21] is applied to separate hydrodynamics from acoustics knowing their different propagation velocities. To apply this filtering, the waves are measured in 3 outlet x-normal planes (instead of just 1) in close proximity. The Taylor hypothesis and the known wave speed are then used to correlate the data between the 3 planes from different physical times following the formula:

$$w_a = \frac{1}{3}\sum_{i=0}^{2} f(x - i\Delta x, t - \frac{i\Delta x}{u_a}) \quad (1)$$

In Eq. (1), f is the wave of interest, w_a is the filtered wave, Δx is the distance between the planes and u_p is the wave speed, i.e $\overline{u} + c$ for w^+ and $\overline{u}$ for w^s.

Results, applying the procedure described above, are summarized in Fig. 9, where they are also compared to the theory and 2D numerical predictions. The 2D and compact theory results are available for a broader range of frequencies. The 3D predictions are close to the 2D ones, while the compact theory predicts stronger upstream propagating generated noise and slightly lower transmitted noise. Regarding the entropy wave transmission, the results of the 3D simulation suggest that at the turbine outlet the injected wave has been dissipated more than in the 2D simulations, while the theoretical approach neglects the entropy wave attenuation process. Concerning the acoustic waves generated at the forcing frequency, for the downstream propagating acoustic wave, the two numerical simulations are in reasonable agreement. For the upstream propagating wave, the 3D simulation predicts a small decrease in strength compared to the 2D prediction, probably because of the choked operating condition that prevents acoustic waves generated downstream the sonic line to propagate towards the turbine inlet.

CONCLUSIONS

The indirect combustion noise generation has been evaluated with LES of a 3D high-pressure turbine stage subjected to a constant-frequency entropy wave train pulsation. To simplify the data processing, the flow field and the generated noise are analyzed through the Dynamic Mode Decomposition of instantaneous snapshots at several positions across the turbine and the results are compared with a steady inflow case. The wave injection generates a distinctive high-amplitude mode at the pulsation frequency, as well as interaction modes with the blade passing frequency. The influence of the entropy waves is also captured by the sparsity-promoting DMD, a modified DMD algorithm that provides an accurate reconstruction of the flow field with few well-selected modes. Despite the presence of broadband turbulence and non-linear interactions, the blade passing frequency and pulsation modes are shown to be the most important ones. For the forced frequency, a detailed analysis of the 3D LES predictions is performed and the results are compared with the compact theory of [6] as well as 2D simulations of a similar turbine configuration. While the theory overpredicts the noise levels, the 3D LES of the choked transonic HP turbine reveals

Copyright © 2015 by ASME

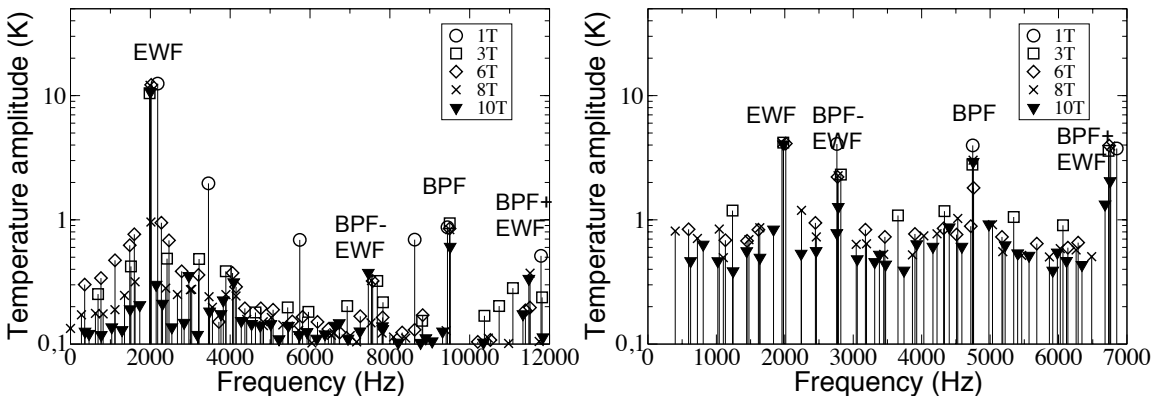

FIGURE 6: DMD TEMPERATURE SPECTRA OF THE PULSED CASE WITH DIFFERENT NUMBER FOR DIFFERENT RUNTIMES - STATOR (LEFT) AND ROTOR DOMAIN (RIGHT) AT MID-SPAN

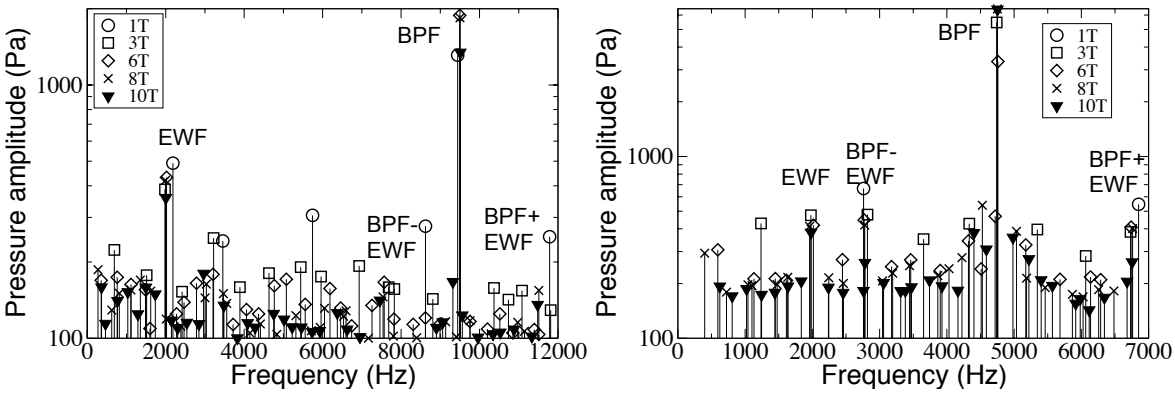

FIGURE 7: DMD PRESSURE SPECTRA OF THE PULSED CASE WITH DIFFERENT NUMBER DIFFERENT RUNTIMES - STATOR (LEFT) AND ROTOR DOMAIN (RIGHT) AT MID-SPAN

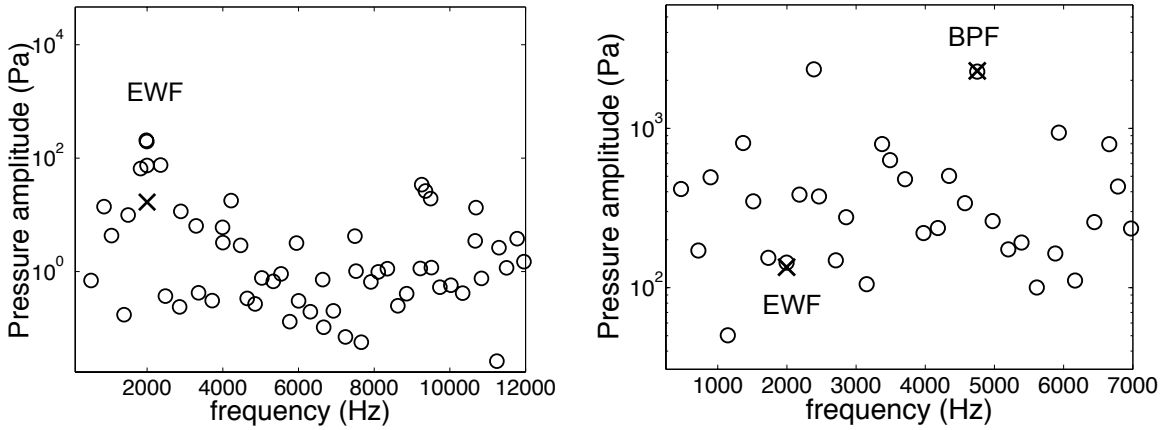

FIGURE 8: SPARSITY-PROMOTING DMD AT THE STATOR INLET (LEFT) AND ROTOR OUTLET (RIGHT) - ORIGINAL DMD MODES ($\circ$) AND SPDMD SELECTED MODES ($\times$)

Copyright © 2015 by ASME

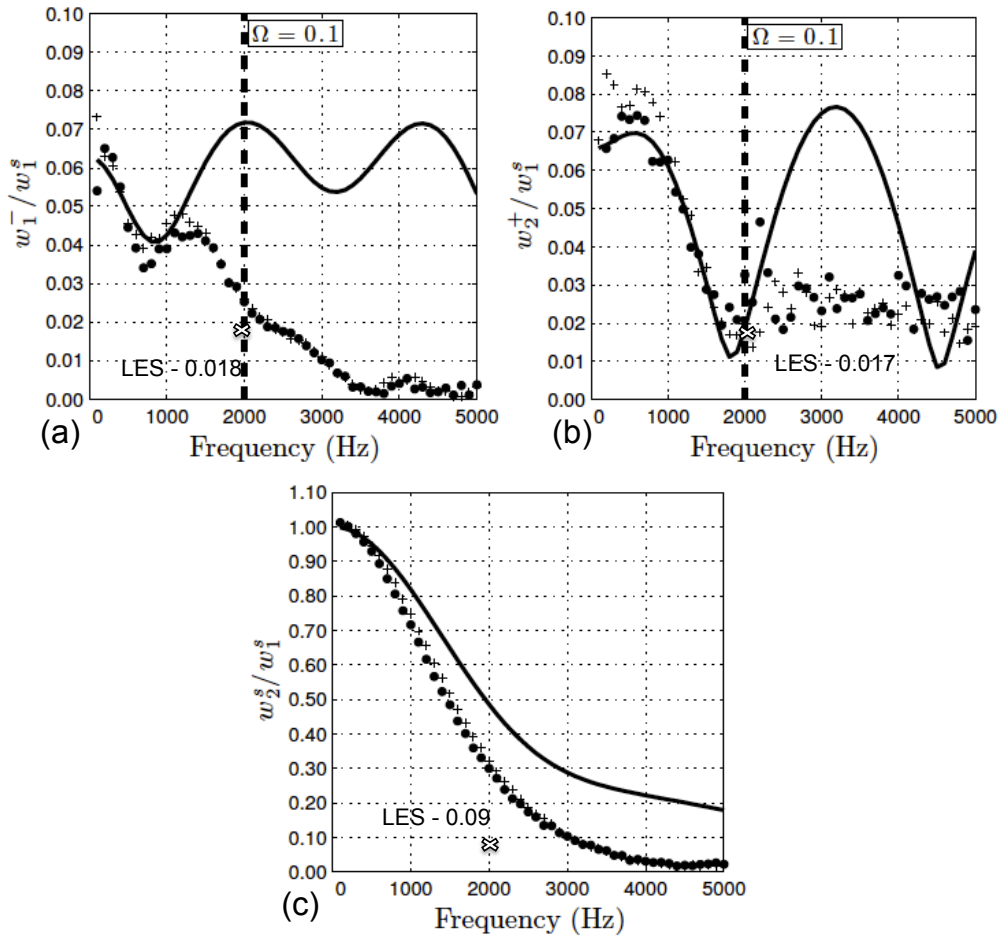

FIGURE 9: COMPARISONS OF THE EVALUATED TRANSMISSION COEFFICIENTS USING 3D LES (×), 2D PREDICTIONS (+ AND •) AND THE COMPACT THEORY (−)

that the entropy waves get highly distorted and weakly transmitted to the following stages than in 2D and in the compact theory (unlikely to generate any additional indirect noise). The transmitted acoustic waves to the consequent stages remain strong, and will equally contribute to the indirect noise as in 2D. The reflected acoustic waves are slightly weaker than in 2D predictions, and much more attenuated than in the compact theory.

ACKNOWLEDGMENT

The authors would like to thank Peter Schmid and Joe Nichols for the fruitful discussions and suggestions on the Dynamic Mode Decomposition. The help of Marlene Sanjosé, Thomas Jaravel, Thomas Livebardon and Michael Bauerheim is gratefully acknowledged. This work was performed using HPC resources from GENCI- [TGCC/CINES/IDRIS] (Grant 2014-x20142b5031) and from Compute Canada.

REFERENCES

[1] Motheau, E., Selle, L., Poinsot, T., and Nicoud, F., 2012. "A mixed acoustic-entropy combustion instability in a realistic gas turbine". In Proc. of the 2012 Summer Program, Center for Turbulence Research.

[2] Marble, F. E., and Candel, S., 1977. "Acoustic disturbances from gas nonuniformities convected through a nozzle". *J. Sound Vib.,* ***55***, pp. 225–243.

[3] Duran, I., and Moreau, S., 2013. "Solution of the quasi one-dimensional linearized euler equations using flow invariants and the magnus expansion". *J. Fluid Mech.,* ***723***, pp. 190–231.

[4] Bake, F., Richter, C., Muhlbauer, B., Kings, N., I.Rohle,

Copyright © 2015 by ASME

F.Thiele, and B.Noll, 2009. "The entropy wave generator (ewg): a reference case on entropy noise". *J. Sound Vib.*, pp. 574–598.

[5] Leyko, M., 2010. "Mise en oeuvre et analyse de calculs aéroacoustiques de type sge pour la prévision du bruit de chambres de combustion aéronautiques". PhD thesis, Institut National Polytechnique de Toulouse.

[6] Cumpsty, N. A., and Marble, F. E., 1977. "The interaction of entropy fluctuations with turbine blade rows; a mechanism of turbojet engine noise". *Proc. R. Soc. Lond. A,* ***357***, pp. 323–344.

[7] Duran, I., and Moreau, S., 2012. "Study of the attenuation of waves propagating through fixed and rotating turbine blades". In 18th AIAA/CEAS Aeroacoustics Conference, pp. AIAA2012–2133.

[8] Duran, I., 2013. "Prediction of combustion noise in modern aero-engines combining large eddy simulations and analytical methods". PhD thesis, Institut National Polytechnique de Toulouse.

[9] Schmid, P., 2010. "Dynamic mode decomposition of numerical and experimental data". *J. Fluid Mech.,* ***656***, pp. 5–28.

[10] Beard, P., Smith, A., and Povey, T., 2011. "Experimental and computational fluid dynamics investigation of the efficiency of an unshrouded transonic high pressure turbine". *J. of Power and Energy,* ***225***, pp. 1166–1179.

[11] Papadogiannis, D., Wang, G., Moreau, S., Duchaine, F., Sicot, F., and Gicquel, L., 2014. "Large eddy simulation of a high-pressure turbine stage: Effects of sub-grid scale modeling and mesh resolution". In Proc. of the ASME Turbo Expo 2014, no. GT2014-25786.

[12] Wang, G., Papadogiannis, D., Duchaine, F., Gourdain, N., and Gicquel, L., 2013. "Towards massively parallel large eddy simulation of turbine stages". In Proceedings of the ASME Turbo Expo 2013 Gas Turbine Technical Congress and Exposition, no. GT2013-64852.

[13] Wang, G., Duchaine, F., Papadogiannis, D., Duran, I., Moreau, S., and Gicquel, L., 2014. "An overset grid method for large eddy simulation of turbomachinery stages". *J. Comput. Phys.,* ***274***, pp. 333–355.

[14] Duchaine, F., Jaure, S., Poitou, D., Quemerais, E., Staffelbach, G., Morel, T., and Gicquel, L., 2013. "High performance conjugate heat transfer with the openpalm coupler". In V International Conference on Coupled Problems in Science and Engineering.

[15] Colin, O., and Rudgyard, M., 2000. "Development of high-order taylor-galerkin schemes for unsteady calculations". *J. Comput. Phys.,* ***162***(2), pp. 338–371.

[16] Nicoud, F., and Ducros, F., 1999. "Subgrid-scale modelling based on the square of the velocity gradient tensor". *Flow, Turb. and Combustion,* ***62***, pp. 183–200.

[17] Poinsot, T., and Lele, S., 1992. "Boundary conditions for direct simulations of compressible viscous flows". *J. Comput. Phys.,* ***101***, pp. 104–129.

[18] Bennett, G., and Fitzpatrick, J., 2008. "Noise source identification for ducted fan systems". *AIAA Journal,* ***46***(7), pp. 1663–1674.

[19] Schmid, P., 2013. "Dynamic mode decomposition". In *VKI Lecture Series*.

[20] Jovanovic, M. R., Schmid, P., and Nichols, J., 2014. "Sparsity-promoting dynamic mode decomposition". *Phys. Fluids,* ***26***(2).

[21] Kopitz, J., Bröcker, E., and Polifke, W., 2005. "Characteristics-based filter for identification of planar acoustic waves in numerical simulation of turbulent compressible flow". In Proceedings of the 12th ICSV.

Copyright © 2015 by ASME